

Pseudo complementary measurement for traditional single-pixel cameras

Qian Dong(董乾), Xu-Ri Yao(姚旭日), Xin Liu(刘歆), Bing Liu(刘冰), Guang-Jie Zhai(翟光杰)

Citation: Chin. Phys. B . 2020, 29(11): 114202 . **doi:** 10.1088/1674-1056/abb22b
Journal homepage: http://cpb.iphy.ac.cn; http://iopscience.iop.org/cpb

What follows is a list of articles you may be interested in

Compressed ghost imaging based on differential speckle patterns

Le Wang(王乐), Shengmei Zhao(赵生妹)

Chin. Phys. B . 2020, 29(2): 024204 . **doi:** 10.1088/1674-1056/ab671a

Proof-of-principle experimental demonstration of quantum secure imaging based on quantum key distribution

Yi-Bo Zhao(赵义博), Wan-Li Zhang(张万里), Dong Wang(王东), Xiao-Tian Song(宋萧天), Liang-Jiang Zhou(周良将), Chi-Biao Ding(丁赤飚)

Chin. Phys. B . 2019, 28(10): 104203 . **doi:** 10.1088/1674-1056/ab3e66

Experimental demonstration of influence of underwater turbulence on ghost imaging

Man-Qian Yin(殷曼倩), Le Wang(王乐), Sheng-Mei Zhao(赵生妹)

Chin. Phys. B . 2019, 28(9): 094201 . **doi:** 10.1088/1674-1056/ab33ee

Mask-based denoising scheme for ghost imaging

Yang Zhou(周阳), Shu-Xu Guo(郭树旭), Fei Zhong(钟菲), Tian Zhang(张天)

Chin. Phys. B . 2019, 28(8): 084204 . **doi:** 10.1088/1674-1056/28/8/084204

Image encryption using random sequence generated from generalized information domain

Xia-Yan Zhang(张夏衍), Guo-Ji Zhang(张国基), Xuan Li(李璇), Ya-Zhou Ren(任亚洲), Jie-Hua Wu(伍杰华)

Chin. Phys. B . 2016, 25(5): 054201 . **doi:** 10.1088/1674-1056/25/5/054201

Pseudo complementary measurement for traditional single-pixel cameras*

Qian Dong(董乾)[1], Xu-Ri Yao(姚旭日)[2,†], Xin Liu(刘歆)[3,4], Bing Liu(刘冰)[2], and Guang-Jie Zhai(翟光杰)[2,4]

[1] *State Key Laboratory of Computer Science, Institute of Software, Chinese Academy of Sciences, Beijing* 100190, *China*
[2] *Key Laboratory of Electronics and Information Technology for Space Systems, National Space Science Center, Chinese Academy of Sciences, Beijing* 100190, *China*
[3] *State Key Laboratory of Scientific and Engineering Computing, Academy of Mathematics and Systems Science, Chinese Academy of Sciences, Beijing* 100190, *China*
[4] *University of Chinese Academy of Sciences, Beijing* 100049, *China*

(Received 25 May 2020; revised manuscript received 8 July 2020; accepted manuscript online 25 August 2020)

A traditional single-pixel camera needs a large number of measurements to reconstruct the object with compressive sensing computation. Compared with the $1/0$ matrices in classical measurement, the $1/-1$ matrices in the complementary measurement has better property for reconstruction computation and returns better reconstruction results. However, each row of the $1/-1$ matrices needs two measurements with the traditional single-pixel camera which results into double measurements compared with the $1/0$ matrices. In this paper, we consider the pseudo complementary measurement which only takes the same amount of measurements with the row number of some properly designed $1/0$ matrix to compute the total luminous flux of the objective and derives the measurement data of the corresponding $1/-1$ matrix in a mathematical way. The numerical simulation and experimental result show that the pseudo complementary measurement is an efficient tool for the traditional single-pixel camera imaging under low measurement rate, which can combine the advantages of the classical and complementary measurements and significantly improve the peak signal-to-noise ratio.

Keywords: computational imaging, single-pixel camera

PACS: 42.30.Va, 42.79.Hp **DOI:** 10.1088/1674-1056/abb22b

1. Introduction

Compressive sensing (CS)[1–5] is very powerful in signal and image processing, which can reduce sampling rate and guarantee reconstruction quality with the sparse property of objects. According to the methodology of CS, a single-pixel camera[6–8] has been built, which has the following structure.

As shown in Fig. 1, the object is imaged onto a digital micro-mirror device (DMD) which consists of individually addressable mirrors, and each mirror can be tilted in two different directions, $+12^{\circ}(1)$ or $-12^{\circ}(0)$ with respect to the surface of the DMD. The incident light from the target is reflected into the two directions depending on the $0/1$ pattern encoded on the DMD and collected into a point detector. Obviously, only non-negative matrices can be directly displayed by DMD in physics.

Compared to traditional optical cameras, the single-pixel camera only uses the one detector to derive much lager luminous flux which can efficiently decrease the signal-to-noise ratio of observed data. With the above characteristic, the single-pixel camera has gotten great success in many optical fields, such as infrared imaging,[9,10] three-dimensional imaging,[11–13] fluorescence microscopy,[14] spectroscopic imaging[15–18] and super-resolution domain imaging.[19–21]

As we introduced above, the traditional single-pixel camera can only measure the flux of partial pixels in the object where the corresponding micro-mirrors turn $+12^{\circ}$ and the corresponding elements in the measurement matrix are 1, which is called the classical measurement. Recently, the complementary measurement single-pixel camera has been proposed in Refs. [22–26], which can derive the two fluxes of the partial pixels in the object simultaneously by two detectors where the corresponding elements in the measurement matrix are 1 and -1, respectively. However, each detector has its own optical characteristic which influences the consistency about the two complementary fluxes and may return unbelievable reconstruction result. Therefore, we focus on the traditional single-pixel camera.

For the traditional single-pixel camera, we can also implement one complementary measurement with obtaining the fluxes of the 1 and -1 parts in the measurement matrix by two measurements, which is called the complementary measurement. No matter we take the classical measurement or the complementary measurement, the measurement matrix includes random,[27–29] Toeplitz[27,28,30] and Hadamard[31–33] matrices.

The measurement matrix is very critical for the reconstruction result. Usually, $1/-1$ matrices in the complementary

*Project supported by the National Key Research and Development Program of China (Grant No. 2018YFB0504302), the Youth Innovation Promotion Association of Chinese Academy of Sciences, and the National Natural Science Foundation of China (Grant Nos. 11701545, 11971466, and 11991021).

†Corresponding author. E-mail: yaoxuri@nssc.ac.cn

© 2020 Chinese Physical Society and IOP Publishing Ltd

measurement outperform $1/0$ matrices in the classical measurement for reconstructing the object with the single-pixel camera under the same sampling rate, which can been seen in the following text. However, as we said above, the sampling number of the former is twice as many as that of the latter when the row number of the measurement matrix is fixed. Therefore, we need compare the performance of the both under same measurement number and consider the improvement of the reconstruction result by some subtly designed measurement matrix.

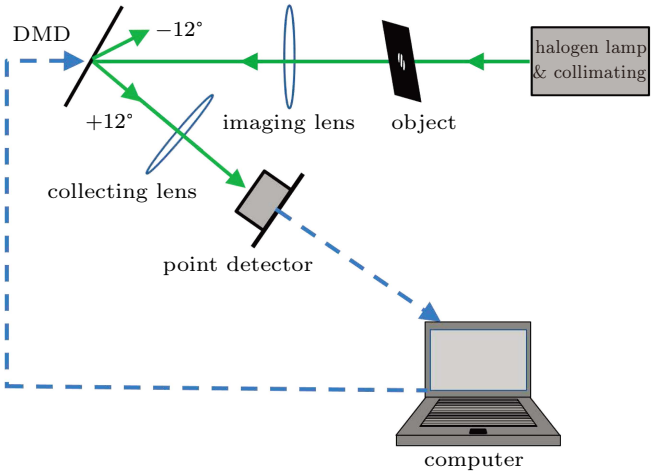


Fig. 1. Single-pixel camera.

The rest of this paper is organized as follows. In Section 2, we introduce the mathematical formulation for the single-pixel camera and show the reconstruction result of the classical and complementary measurements. In Section 3, we propose the pseudo complementary measurement, design certain matrix satisfying some assumptions, and study the properties of that matrix. In Section 4, we show the performance profile and take numerical simulation about our pseudo complementary measurement with some standard testing image. In Section 5, we reconstruct certain object with our pseudo complementary measurement compared with the classical and complementary measurements under the same low measurement rate. In Section 6, we conclude this paper.

2. Comparison between the classical and complementary measurements

The measurement processing of the single-pixel camera can be expressed mathematically in the following way:

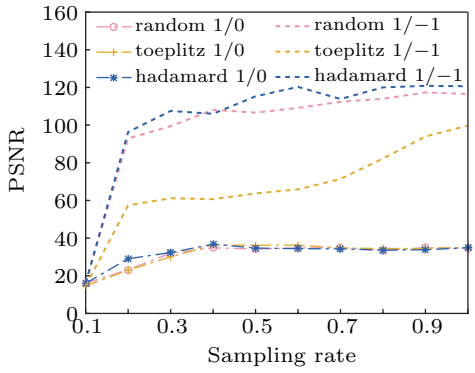
$$b = Au + e, \tag{1}$$

where $u \in \mathbb{R}^n$ is the measured object, $A \in \mathbb{R}^{m\times n}$ is the measurement matrix, $e \in \mathbb{R}m$ is the noise, and $b \in \mathbb{R}m$ is the received data. In Eq. (1), the matrix A usually has fewer rows than columns due to the low sampling rate. Therefore, the above linear system (1) is undetermined. Fortunately, the measured object always has some sparse structures. With this priority knowledge, researchers have proposed many excellent algorithms to reconstruct the object. In this paper, we use TVAL3[34] to solve the above system (1), which is a very efficient solver using the sparseness of the gradient information of the object.

Now we show the reconstruction quality versus sampling rate of different matrices for the 64×64 head phantom picture (Fig. 2(a)) in Matlab. Here we use random, Toeplitz and Hadamard matrices as measurement matrices. All of these matrices are employed in the classical and complementary measurements, which are denoted by the $1/0$ and $1/-1$ matrices, respectively. The Hadamard matrices in this paper are in a random sequence, which means that we take random permutation of the original Hadamard matrices in rows and columns. The sampling rate, i.e., the ration between m and n, is taken from 10% to 100%. Without the influence of noise ($e = \mathbf{0}_m$), we can see that $1/-1$ matrices have much better construction results than $1/0$ matrices under the same sampling rates from Fig. 2(b). This is due to the fact that the off-diagonal components in $A^{\mathrm{T}}A$ for $1/-1$ matrices are close to 0 while those for $1/0$ matrices are about half the diagonal components, which is shown in Fig. 3. The sampling rate in Fig. 3 is 30%. That is to say, the dimension of the matrices in Fig. 3 is 1228×4096. Since the row number is less than the column number, the orthogonality of columns in these matrices can not be guaranteed. However, the inner products of columns in $1/-1$ matrices are close to 0 due to the random property or the characteristic of the Hadamard matrix. When the diagonal components dominate the matrix, we can derive high-quality solution easily in mathematical numerical computation. Consequently, the complementary measurement returns better reconstruction result than the classical measurement.



(a) Head phantom.



(b) PSNR vs sampling rate, noiseless case.

Fig. 2. The reconstruction quality versus sampling rate of different matrices for head phantom picture. In (b), the "random", "toeplitz" and "hadamard" mean the random, Toeplitz and Hadamard matrices, respectively; the "1/0" and "1/−1" mean the $1/0$ and $1/-1$ matrices, respectively. The "hadamard–1/0" matrix is made with the 1 part of the corresponding Hadamard matrix. The sampling rates are taken 0.1, 0.2, 0.3, …, 1.

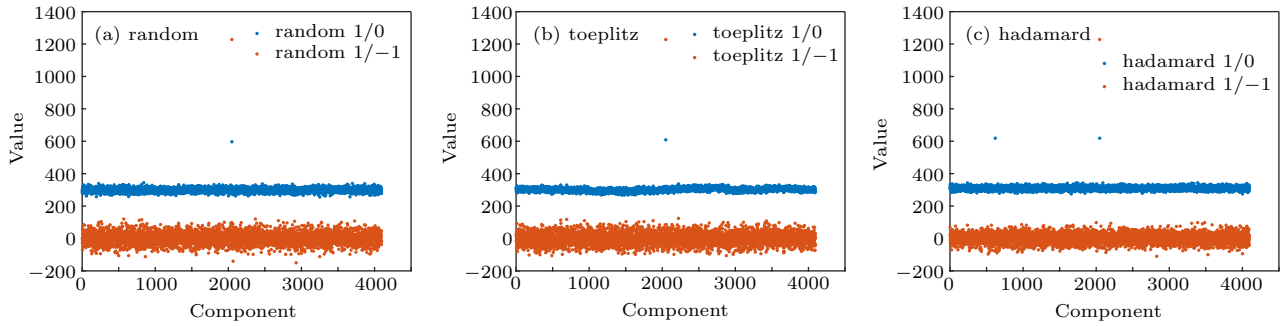


Fig. 3. The components in the 2048th row of $A^{\mathrm{T}}A$ of different matrices, where $A \in \mathbb{R}^{1228\times 4096}$.

However, as we analyzed above, $1/-1$ matrices in the complementary measurement need a doubling of measurements compared with $1/0$ matrices in the classical measurement under the same sampling rate which means the ratio between the row number of the measurement matrix and the pixel number of the object. That is obviously unfair for the classical measurement. Therefore, in this paper, we introduce the measurement rate which respects the ratio between the number of the measurements and the pixel number of the object. Under the same measurement rate, all matrices have the same number of measurements with the single-pixel camera. Specifically, with the same measurement rate, the number of the complementary sampling, i.e., the row number of $1/-1$ matrices, become half of the number of classical sampling, i.e., the row number of $1/0$ matrices.

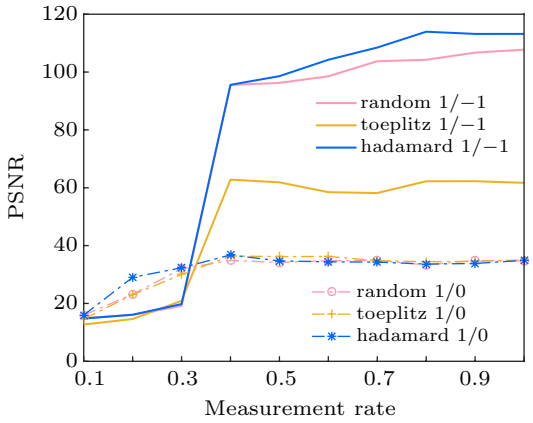


Fig. 4. Peak signal-to-noise ratio (PSNR) vs measurement rate of different measurements (matrices), noiseless case. The legends are the same as the ones in Fig. 2. The measurement rates are taken as 0.1, 0.2, 0.3, ..., 1.

Now we compare the reconstruction quality versus the measurement rate of different measurements (matrices) shown in Fig. 4. Figure 4 shows that with low measurement rate (about less than 30%) the classical measurement ($1/0$ matrices) can actually reconstruct the object better than the complementary measurement ($1/-1$ matrices) and only if the measurement rate is enough large (about greater than 40%) the complementary measurement can return better results than the classical measurement. The performance of the complementary measurement motivates us to consider how to improve the imaging quality of the single-pixel camera under low measurement rate.

3. Pseudo complementary measurement

In the above section, we find that $1/-1$ matrices in the complementary measurement have better reconstruction results than $1/0$ matrices in the classical measurement with the single-pixel camera but the true measurement number of $1/-1$ matrices are twice $1/0$ matrices under the same sampling rate. Those facts drive us to study the implementation about the complementary measurement of $1/-1$ matrices just with the same measurement number of the classical measurement.

3.1. Basic idea

The complementary measurement processing has the following mathematical formulation:

$$b_+ = A_+u + e_+, \tag{2}$$

$$b_- = A_-u + e_-, \tag{3}$$

where

$$A_+ = \frac{1}{2}(A + \mathbf{1}_{m\times n}), \tag{4}$$

$$A_- = \frac{1}{2}(\mathbf{1}_{m\times n} - A), \tag{5}$$

and $e_+ \in \mathbb{R}m$ and $e_- \in \mathbb{R}m$ respect the noises in $b_+ \in \mathbb{R}m$ and $b_- \in \mathbb{R}m$, respectively. As Eqs. (2) and (3), the traditional single-pixel camera receives two fluxes b_+ and b_- corresponding to 1 and -1 elements in the matrix A. According to Eqs. (4) and (5), we obtain

$$Au = (A_+u - A_-u). \tag{6}$$

Combining Eqs. (4) and (5), we have

$$A_- = \mathbf{1}_{m\times n} - A_+. \tag{7}$$

From Eqs. (6) and (7), we derive

$$Au = 2A_+u - F_u\mathbf{1}_m, \tag{8}$$

where $F_u = u^{\mathrm{T}}\mathbf{1}_n$ respects the total flux of the object. Equation (8) provides us one way to derive the term b only with the

same number of measurement with the row number of the matrix A if we can estimate the total luminous flux of the object. We call Eq. (8) the pseudo complementary measurement since the complementary measurement receives both A_+u and A_-u, but in Eq. (8) we only need A_+u.

3.2. Assumptions on the matrix A_+

In tradition, the total flux is computed by the summation of all pixel values of the image in numerical simulation and measured through turning all micro-mirrors $+12^\circ$ in real experiment. If we just measure the total luminous flux once, its value is seriously affected by the measurement error. Based on the statistical theory, we can take several times measurements to derive the accurate value of total flux. Fortunately, we find that certain part of the total luminous flux F_u can be derived in each measurement based on Eq. (1). If we can design the measurement matrix properly, the total luminous flux F_u can be computed easily in a mathematical way. Therefore, we consider the following assumption on the matrix A_+ to obtain the total luminous flux F_u from A_+u.

Assumption 1 The matrix A_+ satisfies

$$A_+^{\mathrm{T}}\mathbf{1}_m = \frac{m}{2}\mathbf{1}_n. \tag{9}$$

Assumption 1 essentially requires that half of the elements in each column of the matrix A_+ is 1. With Assumption 1, we immediately derive the following lemma.

Lemma 1 Suppose Assumption 1 holds. Then it holds that

$$(A_+u)^{\mathrm{T}}\mathbf{1}_m = \frac{m}{2}F_u. \tag{10}$$

Proof From the matrix vector multiplication, we have

$$(A_+u)^{\mathrm{T}}\mathbf{1}_m = u^{\mathrm{T}}(A_+^{\mathrm{T}}\mathbf{1}_m) = \frac{m}{2}u^{\mathrm{T}}\mathbf{1}_n = \frac{m}{2}F_u.$$

It is easily seen that Lemma 1 provides us one way to obtain the total flux F_u based on the measured data. According to Lemma 1, the pseudo complementary measurement (8) under Assumption 1 is equivalent to

$$Au = 2(A_+u - \overline{A_+u}\mathbf{1}_m), \tag{11}$$

where $\overline{A_+u} = \frac{1}{m}(A_+u)^{\mathrm{T}}\mathbf{1}_m$ respects the mean value of measured fluxes. Obviously, we can see that the pseudo complementary measurement (11) only takes the measurement about A_+u and does not need A_-u.

In this paper, we also suppose that the matrix A_+ satisfies the following assumption.

Assumption 2 The matrix A_+ satisfies

$$A_+\mathbf{1}_n = \frac{n}{2}\mathbf{1}_m. \tag{12}$$

Assumption 2 essentially requires that half of the elements in each row of the matrix A_+ is 1. With Assumption 2, we immediately derive the following lemma.

Lemma 2 Suppose Assumption 2 holds. Then it holds that

$$A\mathbf{1}_n = \mathbf{0}_m. \tag{13}$$

Proof From Eq. (4), we have that

$$A\mathbf{1}_n = (2A_+ - \mathbf{1}_{m\times n})\mathbf{1}_n = \mathbf{0}_m.$$

We can see that if the matrix A_+ satisfies Lemma 2, the matrix A can remove the direct-current component and only keep the difference of the measured object.

3.3. Matrix design for the pseudo complementary measurement

Assumptions 1 and 2 require that the half of elements in both each row and each column are 1, which can be generated in Algorithm 1.

Algorithm 1: Matrix generation based on Assumptions 1 and 2

1 Generate the $1/0$ random matrix A_+ which has $m/2$ 1s in each column.
2 Compute and sort the quantity of 1s in each row. If the smallest value is equal to $n/2$, the algorithm ends.
3 Switch 0 and 1 at the random column in the two rows which have the smallest and largest value respectively.
4 Go to Step 2.

The step 1 in Algorithm 1 guarantees each column of the matrix A_+ has half of 1s as the row number of A_+. The step 2 and 3 only adjust the distribution of 1s among rows of A_+ and keep the number of 1s in each column $\frac{m}{2}$. With executing the step 2 and 3 once, the difference between the smallest and largest quantity of 1s in each row will decrease. Consequently, Algorithm 1 can be terminated with finite steps, which is concluded in the following theorem.

Algorithm 1 can generate the matrix A_+ satisfying Assumption 1 and 2 within finite steps.

For the large-scale matrix, we can generate it from the small-scale matrix based on the following lemma.

Lemma 3 Suppose that the matrix $A_0 \in \mathbb{R}^{m\times n}$ satisfies Assumption 1 and 2. It holds that the following matrix A_1 generated from A_0 also satisfies Assumption 1 and 2,

$$A_1 = \begin{pmatrix} A_0 & A_0 \\ A_0 & \mathbf{1}_{m\times n} - A_0 \end{pmatrix}.$$

Proof With the block matrix vector multiplication, we have

$$A_1\mathbf{1}_{2n} = (2A_0\mathbf{1}_n, n\mathbf{1}_m)^{\mathrm{T}} = n\mathbf{1}_{2m},$$
$$A_1^{\mathrm{T}}\mathbf{1}_{2m} = (2A_0^{\mathrm{T}}\mathbf{1}_m, m\mathbf{1}_n)^{\mathrm{T}} = m\mathbf{1}_{2n}.$$

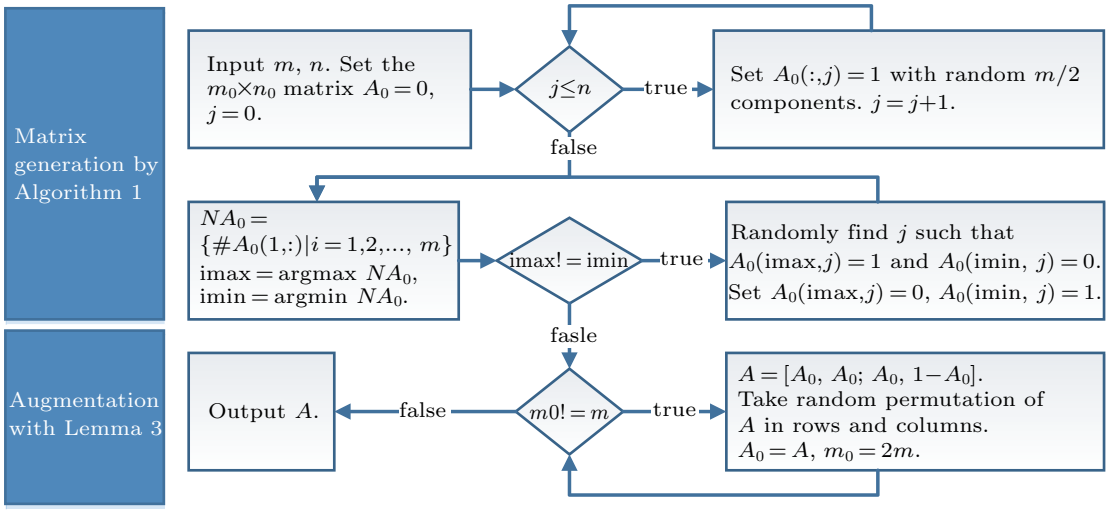


Fig. 5. The flow chart based on Algorithm 1 and Lemma 3.

Combing Algorithm 1 and Lemma 3, we can build a flow chart about the matrix generation for the pseudo complementary measurement as shown in Fig. 5. First, we initialize a small-scale matrix just satisfying Assumption 1. Then we switch 0 and 1 in the same column from the rows having the smallest and largest amount of 1s respectively in order to make the small-scale matrix satisfy Assumption 2. Finally, we augment the initial matrix in rows and columns recurrently to obtain the desired matrix.

3.4. Computational property and error analysis for the pseudo complementary measurement

The designed matrix by Algorithm 1 has the similar property with the random matrix. Here we first generate a $\mathbb{R}^{306\times1024}$ matrix, and then we extend the matrix double and four times in size based on Lemma 3. From Fig. 6, we can see that the matrix A designed by Algorithm 1 for the pseudo complementary measurement has the similar computational property with 1/−1 matrices for the complementary measurement shown in Fig. 3. Therefore, we believe that our new matrix with the pseudo complementary measurement can have good performance for reconstructing the object with the single-pixel camera.

Now we consider the error analysis of the pseudo complementary measurement. Suppose that $e_+, e_- \sim N(\mathbf{0}_m, \sigma^2 I_{m\times m})$ and e_+ and e_- are independent of each other. According to Eqs. (2) and (11), we have

$$\begin{aligned} b &= 2(b_+ - \overline{b_+}\mathbf{1}_m) = 2(A_+u + e_+ - (\overline{A_+u} + \overline{e_+})\mathbf{1}_m) \\ &\approx 2(A_+u - \overline{A_+u}\mathbf{1}_m) + 2e_+. \end{aligned} \tag{14}$$

The approximation in Eq. (14) is due to the fact that $e_+ \sim N(\mathbf{0}_m, \sigma^2 I_{m\times m})$ and m is large enough, which results in $\overline{e_+} \approx 0$ with the statistical theory, which means that the total flux F_u can be estimated by $\overline{A_+u}$ accurately. For the complementary measurement, we have

$$b = (b_+ - b_-) = (A_+u - A_-u) + e_+ - e_-. \tag{15}$$

Since $2e_+ \sim N(\mathbf{0}_m, 4\sigma^2 I_{m\times m})$ and $e_+ - e_- \sim N(\mathbf{0}_m, 2\sigma^2 I_{m\times m})$, combining Eqs. (14) and (15), the ratio about the standard deviation of noises between the pseudo complementary and complementary measurements is $\sqrt{2}$. In addition, based on Eq. (14), the ratio about the standard deviation of noises between the pseudo complementary and classical measurements is 2. That is to say, the noise level for the pseudo complementary measurement is similar to the classical and complementary measurements.

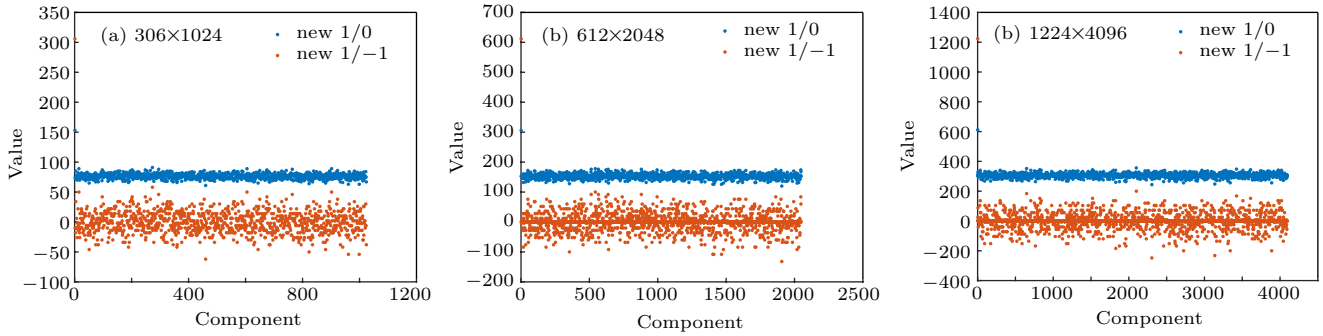


Fig. 6. The components in the 1st row of $A^{\mathrm{T}}A$ of the matrices. The dimension of A is listed in the sub-figures. The "new–1/0" matrix is designed by Algorithm 1 and Lemma 3, and the "new–1/−1 matrix" is computed based on Eq. (4).

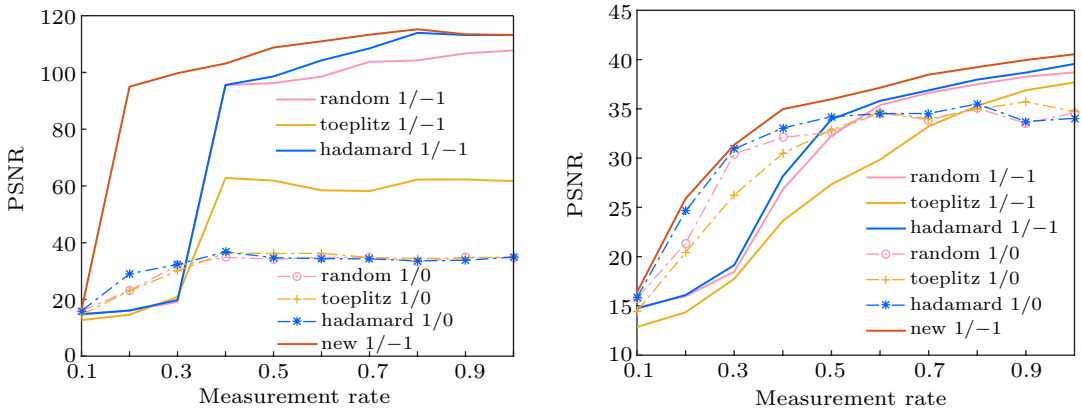
4. Numerical simulation

In this section, we first draw the figure about performance profile of the pseudo complementary measurement to compare it with the classical and complementary measurements. Then we show the reconstructed images.

4.1. Performance profile of the pseudo complementary measurement

Now we reconstruct the 64×64 head phantom picture (Fig. 2(a)) with the pseudo complementary measurement. Here we generate the data b followed by Eqs. (2), (3), (14), and (15). Then we take the reconstruction computation and obtain Fig. 7.

For the noiseless case, we can see that under low measurement rates (about less than 30%) the pseudo complementary measurement rapidly improves the construction quality of the complementary measurement. For the noise case ($\sigma = 1$), which is close to the real experimental situation, the pseudo complementary measurement has the best reconstruction quality. In both the noiseless and noise cases, the pseudo complementary measurement overcomes the poor reconstruction quality of the complementary measurement under low measurement rate with the single-pixel camera. Figure 7 shows that the pseudo complementary measurement can combine the advantages of the classical and complementary measurements and give the robust reconstructed results under different measurement rates.

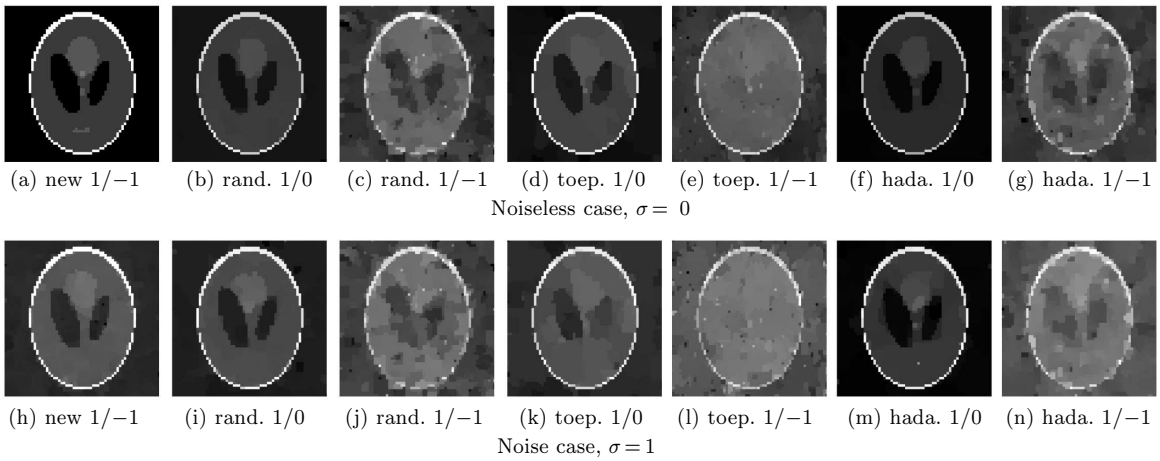


(a) Noiseless case. (b) Noise case, $\sigma = 1$.

Fig. 7. PSNR vs measurement rate with the pseudo complementary measurement. The "new–1/−1" matrix is generated by Algorithm 1 and the other legends are the same as the ones in Fig. 4. The measurement rates are taken as 0.1, 0.2, 0.3, ..., 1.

4.2. Reconstructed image comparisons

In this subsection, we show the reconstructed images under 30% measurement rate in the above subsection with Fig. 7. Since the resolution ratio of the original image is 64×64, the measurement number in Table 1 is 1228, which means that each of the sub-figures except (a) and (i) is reconstructed by 1228 measurements with the virtual traditional signal-pixel camera. In detail, the row number of the pseudo complementary and classical measurements, which include "new 1/−1", "rand. 1/0", "toep. 1/0" and "hada. 1/0" in Table 1, is 1228; the row number of the complementary measurements, which include "rand. 1/−1", "toep. 1/−1" and "hada. 1/−1" in Table 1, is 614 due to the two measurements about the fluxes of the 1 and −1 parts in each row of the 1/−1 matrix.



(a) new 1/−1 (b) rand. 1/0 (c) rand. 1/−1 (d) toep. 1/0 (e) toep. 1/−1 (f) hada. 1/0 (g) hada. 1/−1

Noiseless case, $\sigma = 0$

(h) new 1/−1 (i) rand. 1/0 (j) rand. 1/−1 (k) toep. 1/0 (l) toep. 1/−1 (m) hada. 1/0 (n) hada. 1/−1

Noise case, $\sigma = 1$

Fig. 8. The reconstructed image of the head phantom in Fig. 2(a). Here the measurement rate is 0.3, and σ is the standard deviation of the noise. The "new 1/−1" matrix is generated by Algorithm 1; the "rand.", "toep." and "hada." mean the random, Toeplitz and Hadamard matrix respectively; the "1/0" and "1/−1" mean the 1/0 and 1/−1 matrices, respectively.

Table 1. The reconstructed PSNR of the head phantom in Fig. 1(a).

σ	new $1/-1$	rand. $1/0$	rand. $1/-1$	toep. $1/0$	toep.$1/-1$	hada. $1/0$	hada. $1/-1$
0	**99.74**	31.98	19.16	30.01	20.89	32.31	19.77
1	**31.35**	30.42	18.46	26.25	17.74	30.94	19.13

From Fig. 8, we can see that the reconstruction results of the pseudo complementary measurement ("new $1/-1$") are visibly better than the others. For the noiseless case ($\sigma = 0$), the reconstructed image by the pseudo complementary measurement is very close to the original one and every detail in "new $1/-1$" is correct. For the noise case ($\sigma = 1$), the reconstructed image by the pseudo complementary measurement can give most of the details of the original one but the others like "rand. $1/0$" and "hada. $1/0$" in Fig. 8 even give some wrong details. From Fig. 8, we can obviously see the effective performance of the pseudo complementary measurement for both noiseless and noise cases compared with the classical and complementary measurements.

5. Experimental result

In this section, we use the traditional single-pixel camera to observe 3 alternating opaque and transparent stripes with the different measurements under 30% measurement rate. The experimental setup is given in Fig. 1. The illumination source is a halogen lamp with the central wavelength of 550 nm. The object to be imaged in transmission is Group 2, Element 2 portion of the standard U.S. Air Force (USAF) resolution target, and it is imaged onto the DMD using an achromatic imaging lens ($f = 50.4$ mm). The DMD consists of a 1024×768 array of individually addressable mirrors, and the size of each mirror is 13.68×13.68 μm. An area on the DMD in the window of size 876×876 μm (64×64 piexls) is employed to provide binary patterns on the object plane. In this experiment, a charge-coupled device (CCD, IMPERX 1620M) camera plays as a bucket detector to measure the total intensity transmitted from the object.

The resolution ratio of the original image in the experiment is 64×64. Similar to our numerical simulation, the measurement number of all types of measurements with the single-pixel camera is 1228. That is to say, for the pseudo complementary measurement ("new $1/-1$" in Table 2), we take 1228 times measurements to obtain the fluxes of the 1 part in each row of the $1/0$ matrix and estimate the total flux of the objective by doubling the average of the receive data; for the classical measurement ("rand. $1/0$", "toep. $1/0$" and "hada. $1/0$" in Table 2), we only take 1228 times measurements to obtain the fluxes of the 1 part in each row of the $1/0$ matrix; for the complementary measurement ("rand. $1/-1$", "toep. $1/-1$" and "hada. $1/-1$" in Table 2), we take 614 times measurements to obtain the fluxes of the 1 part in each row of the $1/-1$ matrix and another 614 times measurements to obtain the fluxes of the -1 part in each row of the same $1/-1$ matrix.

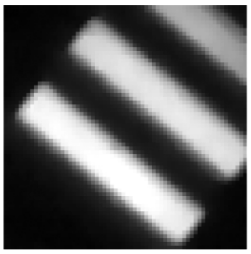


Fig. 9. The original image in the experiment.

After collecting the data, we take the reconstruction computation and derive Table 2 and Fig. 10, from which we can obviously see that the pseudo complementary measurement has the best reconstruction result. The image in "new $1/-1$" derived by our pseudo complementary measurement is the closest to the original one and has clear 3 stripes. Table 2 and Fig. 10 also show that the pseudo complementary measurement has the huge advantage for reconstructing the object under low measurement rate with the traditional single-pixel camera compared with the classical and complementary measurement.



(a) new $1/-1$ (b) rand. $1/0$ (c) rand. $1/-1$ (d) toep. $1/0$ (e) toep. $1/-1$ (f) hada. $1/0$ (g) hada. $1/-1$

Fig. 10. The reconstructed image of Fig. 9. Here the measurement rate is 0.3. The "new $1/-1$" matrix is generated by Algorithm 1; the "rand.", "toep." and "hada." mean the random, Toeplitz and Hadamard matrix respectively; the "$1/0$" and "$1/-1$" mean the $1/0$ and $1/-1$ matrices, respectively.

Table 2. The reconstructed PSNR of Fig. 2(a).

	new $1/-1$	rand. $1/0$	rand. $1/-1$	toep. $1/0$	toep.$1/-1$	hada. $1/0$	hada. $1/-1$
PSNR	**26.49**	14.27	13.97	11.65	12.11	14.64	14.02

6. Conclusions

In summary, we have proposed a pseudo complementary measurement for a traditional single-pixel camera. The noise of this procedure can be guaranteed in the same level with the classical and complementary measurements. With the properly designed measurement matrix, the pseudo complementary measurement can obtain the total luminous flux of the object and construct the received data b for that matrix. The performance of the pseudo complementary measurement in the numerical simulation is better than the classical and complementary measurements under the same measurement rates, which shows that the pseudo complementary measurement can combine the advantages of the classical and complementary measurements under different measurement rates. The experimental result shows that the pseudo complementary measurement can improve the peak signal-to-noise ratio (PSNR) significantly for the traditional single-pixel camera imaging under low measurement rate.

References

[1] Candès E J, Romberg J and Tao T 2006 *IEEE Trans. Inform. Theory* **52** 489
[2] Donoho D L 2006 *IEEE Trans. Inform. Theory* **52** 1289
[3] Candès E J 2006 *Proceedings of the International Congress of Mathematicians*, Madrid, Spain Vol. 3 p. 1433
[4] Candès E J 2008 *Comptes Rendus Mathematique* **346** 589
[5] Romberg J 2008 *IEEE Signal Process. Magaz.* **25** 14
[6] Takhar D, Laska J, Wakin M B, Duarte M F, Baron D, Sarvotham S, Kelly K and Baraniuk R G 2006 *IS&T/SPIE Computational Imaging IV* **6065** 606509
[7] Duarte M F, Davenport M A, Takbar D, Laska J N, Sun T, Kelly K F and Baraniuk R G 2008 *IEEE Signal Process. Magaz.* **25** 83
[8] Chan, W L, Charan K, Takhar D, Kelly K F, Baraniuk R G and Mittleman D M 2008 *Appl. Phys. Lett.* **93** 121105
[9] Radwell N, Mitchell K J, Gibson G M, Edgar M P, Bowman R and Padgett M J 2014 *Optica* **1** 285
[10] Edgar M P, Gibson G M, Bowman R W, Sun B, Radwell N, Mitchell K J, Welsh S S and Padgett M J 2015 *Sci. Rep.* **5** srep10669
[11] Howland G A, Dixon P B and Howell J C 2011 *Appl. Opt.* **50** 5917
[12] Sun M, Edgar M, Gibson G, Sun B, Radwell N, Lamb R N and Padgett M J 2016 *Nat. Commun.* **7** 12010
[13] Li F, Chen H, Pediredla A, Yeh C, He K, Veeraraghavan A and Cossairt O 2017 *Opt. Express* **25** 31096
[14] Studer V, Bobin J, Chahid M, Mousavi H S, Candès J and Dahan M 2012 *Proc. Natl. Acad. Sci. USA* **109** E1679
[15] August Y, Vachman C, Rivenson Y and Stern A 2013 *Appl. Opt.* **52** D46
[16] Arce G R, Brady D J, Carin L, Arguello H and Kittle D S 2014 *IEEE Signal Process. Magaz.* **31** 105
[17] Liu X, Yu W, Yao X, Dai B, Li L, Wang C and Zhai G 2016 *Opt. Commun.* **365** 173
[18] Wang C, Liu X, Yu W, Yao X, Zheng F, Dong Q, Lan R, Sun Z and Zhai G 2017 *Chin. Phys. Lett.* **34** 104203
[19] Gong W and Han S 2012 *Phys. Lett. A* **376** 1519
[20] Yao X, Li L, Liu X, Yu W and Zhai G 2015 *Chin. Phys. B* **24** 044203
[21] Wang P, Li W, Wang C, Bo Z and Gong W 2018 *Chin. Phys. B* **27** 074202
[22] Yu W, Liu X, Yao X, Wang C, Zhai Y and Zhai G 2014 *Sci. Rep.* **4** 5834
[23] Ferri F, Magatti D, Lugiato L A and Gatti A 2010 *Phys. Rev. Lett.* **104** 253603
[24] Sun B, Welsh S S, Edgar M P, Shapiro J H and Padgett M J 2012 *Opt. Express* **20** 16892
[25] Soldevila F, Clemente P, Tajahuerce E, Uribe-Patarroyo N, Andrès P and Lancis J 2016 *Sci. Rep.* **6** 29181
[26] Bian L, Suo J, Dai Q and Chen F 2018 *J. Opt. Soc. Am. A* **35** 78
[27] Zhang G, Jiao S, Xu X and Wang L 2010 *IEEE International Conference on Information and Automation (ICIA)* p. 455
[28] Do T T, Tran T D and Gan L 2008 *IEEE International Conference on Acoustics, Speech and Signal Processing* p. 3369
[29] Monajemi H, Jafarpour S, Gavish M, Collaboration S C and Donoho D L 2013 *Proc. Natl. Acad. Sci. USA* **110** 1181
[30] Tsaig Y and Donoho D L 2006 *Signal Process.* **86** 549
[31] Bajwa W U, Haupt J D, Raz G M, Wright S J and Nowak R D 2007 *IEEE/SP 14th Workshop on Statistical Signal Processing* p. 294
[32] Rauhut H arXiv:0902.4394 [cs.IT]
[33] Sebert F, Zou Y and Ying L 2008 *IEEE ITAB International Conference on Information Technology and Applications in Biomedicine* p. 47
[34] Li C, Yin W, Jiang H and Zhang Y 2013 *Comput. Optim. Appl.* **56** 507